Digital Signal Processing 47 (2015) 169–177

Contents lists available at ScienceDirect

Digital Signal Processing

www.elsevier.com/locate/dsp

Bayesian classification and analysis of gait disorders using image and depth sensors of Microsoft Kinect

Aleš Procházka [a,b,*], Oldřich Vyšata [c], Martin Vališ [c], Ondřej Ťupa [a], Martin Schätz [a], Vladimír Mařík [b]

[a] Department of Computing and Control Engineering, Institute of Chemical Technology in Prague, Czech Republic
[b] Czech Institute of Informatics, Robotics and Cybernetics, Czech Technical University in Prague, Czech Republic
[c] Department of Neurology, Charles University in Prague, Faculty of Medicine, Hradec Králové, Czech Republic

ARTICLE INFO

Article history:
Available online 27 May 2015

Keywords:
Gait recognition
MS Kinect
Three-dimensional modeling
Bayesian classification
Decision boundary
Parkinson's disease

ABSTRACT

This paper presents a novel method of Bayesian gait recognition using Microsoft (MS) Kinect image and depth sensors and skeleton tracking in three-dimensional space. Although video sequences acquired by a complex camera system enable a very precise data analysis, it is possible to use much simpler technical devices to analyze video frames with sufficient accuracy for many applications. The use of the MS Kinect allows a simple 3-D modeling using its image and depth sensors for data acquisition, resulting in a matrix of 640×480 elements used for spatial modeling of a moving body. The experimental part of the paper is devoted to the study of three data sets: (i) 18 individuals with Parkinson's disease, (ii) 18 healthy age-matched controls, and (iii) 15 trained young individuals forming the second reference set. The proposed algorithm involves methods for the estimation of the average stride length and gait speed of individuals in these sets. Digital signal processing methods and Bayesian probability classification algorithms are then used for gait feature analysis to recognize individuals suspected of having Parkinson's disease. The results include the estimation of the characteristics of selected gait features for patients with Parkinson's disease and for individuals from the reference sets, presentation of decision boundaries, and comparison of classification efficiency for different features. The achieved accuracy of the probabilistic classification was 94.1%.

1. Introduction

Pattern recognition [1,2] is a very common problem with many applications in engineering and biomedicine. The Bayesian approach to object tracking [3–5], image separation [6] and classification forms an important part of this area with specific ideas on Bayesian statistical methodology in signal processing developed by professor Bill Fitzgerald [7] from the Engineering Department of the University of Cambridge (UK).

This contribution is devoted to the analysis of gait disorders [8,9] and selected Parkinson's disease attributes [10–12] using the MS Kinect and three-dimensional modeling to detect movement patterns and to subject these features to a Bayesian classification [13,14]. Synchronized video-camera systems [15–17] enable a precise but also expensive technical solution to motion tracking. The present paper shows the alternative application of much cheaper systems using image and depth sensors to acquire data with sufficient accuracy for many areas.

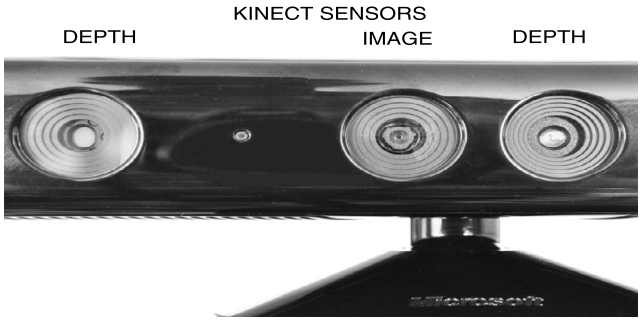

Fig. 1. Location of MS Kinect image and depth sensors used for data acquisition.

The MS Kinect presented in Fig. 1 allows us to record data sets that can be further processed in the appropriate mathematical environment using methods and algorithms for motion anal-

* Corresponding author at: Department of Computing and Control Engineering, Institute of Chemical Technology in Prague, Czech Republic.
E-mail address: A.Prochazka@ieee.org (A. Procházka).

http://dx.doi.org/10.1016/j.dsp.2015.05.011
1051-2004/

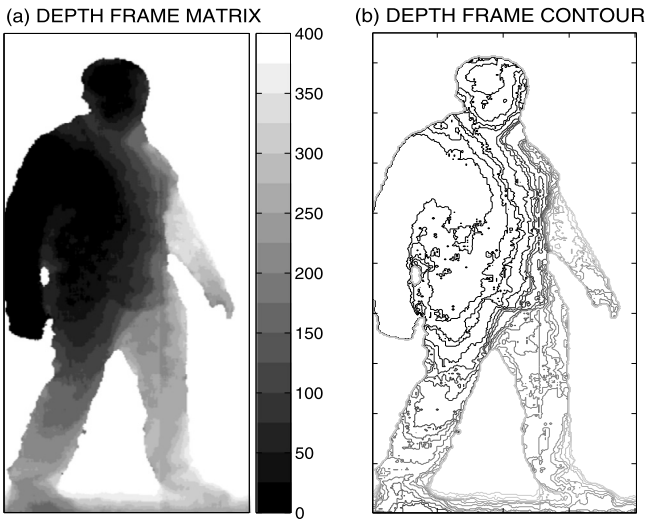

Fig. 2. A selected record obtained from the MS Kinect depth sensor presenting (a) the sample frame with the grey-scale bar of distances [mm] of the individual from the selected plane and (b) the contour plot of the depth matrix.

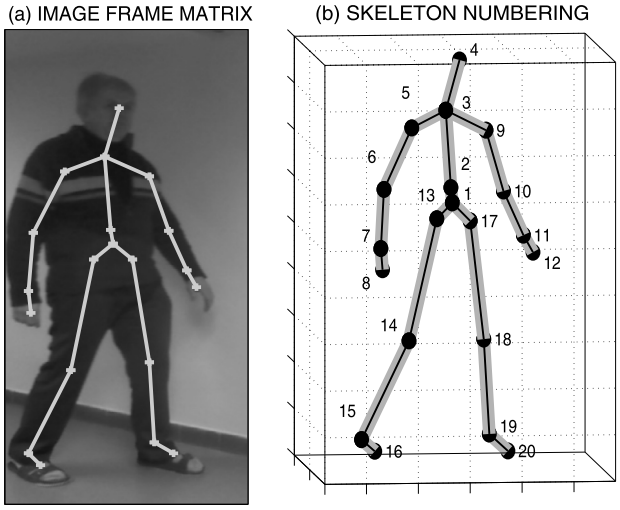

Fig. 3. A selected image recorded by the MS Kinect presenting (a) the sample frame with the image and skeleton and (b) the skeleton with numbering of joints.

ysis [9,18–20], gesture recognition [21] and robotic systems control [22,23]. Selected data acquired from image and depth sensors are presented in Figs. 2 and 3. The skeleton tracking algorithm [24] processes these data to provide information about the location of the joints specified in Fig. 3(b) using the joint numbering and the connection map presented in Table 1. The following mathematical methods are then applied for the motion feature classification and for Parkinson's disease (PD) study.

Recent studies [25,26] indicate that the MS Kinect has the potential to be an inexpensive device for following, with some limitations, movement features and for analyzing the movement symptoms of individuals with gait disorders and Parkinson's disease. Data processing can result in the discrimination of gait patterns, movements of joints, and analysis of gait speed [12] as features characteristic for normal and pathological gait. The whole system can be used in the home environment to follow the worsening of movement symptoms with disease progression or improvements due to intervention.

The present paper proposes using Bayesian classification methods for the analysis of three sets of individuals and for the probabilistic classification of the individuals according to their detected

Table 1
Skeleton positions and connection map of a standing individual used for data acquisition and processing of video records.

Skeleton positions		Skeleton positions	
Joint	No.	Joint	No.
Hip center	1	Wrist right	11
Spine	2	Hand right	12
Shoulder center	3	Hip left	13
Head	4	Knee left	14
Shoulder left	5	Ankle left	15
Elbow left	6	Foot left	16
Wrist left	7	Hip right	17
Hand left	8	Knee right	18
Shoulder right	9	Ankle right	19
Elbow right	10	Foot right	20

Connection map	
Part	Connection vectors
Spine	[1 2], [2 3], [3 4]
Left hand	[3 5], [5 6], [6 7], [7 8]
Right hand	[3 9], [9 10], [10 11], [11 12]
Left leg	[1 13], [13 14], [14 15], [15 16]
Right leg	[1 17], [17 18], [18 19], [19 20]

gait features. This approach, that of statistical pattern recognition and machine learning [27], is based upon initial studies of Thomas Bayes (1701–1761) and modern statistical methods forming the main part of present digital signal processing methods [28–33]. The present paper contributes to the use of these algorithms in biomedicine [34–37] and shows their application in the diagnostics of movement disorders.

2. Methods

2.1. Data acquisition

The MS Kinect system presented in Fig. 1 was used for synchronized data acquisition and spatial modeling [38–43]. The depth sensor of the MS Kinect consists of an infrared projector and an infrared camera (on the left and right of Fig. 1 respectively) that uses the structured light principle [44,45]. The detected distance of sensor pixels acquired with a precision of 4–40 mm (depending upon the distance from the sensor) was then stored in the appropriate elements of a matrix having 480×640 elements. The second sensor, an RGB camera, allowed image data acquisition into another matrix of the same size of 480×640 pixels in each video frame with a sample image presented in Fig. 3(a).

The MATLAB image acquisition toolbox includes tools for the direct interconnection of the MS Kinect and the computer environment. A selected depth frame is presented in Fig. 2(a) together with the grey-scale bar of distances from the plane in the selected distance of 2000 mm in front of MS Kinect, perpendicular to the infrared projector beam. Fig. 2(b) presents contours associated with the distance of the body from the depth sensor. The skeleton detected by MS Kinect sensors is shown both in Fig. 3(a) together with the image frame and in Fig. 3(b) with the numbering of the individual joints presented in Table 1.

The experimental part of the study was devoted to the gait analysis of three sets of individuals of different mean ages and standard deviations (STD) summarized in Table 3, which included: (i) 18 patients (52–87 years old, mean: 73.8, STD: 9.4) with Parkinson's disease, (ii) 18 healthy age-matched individuals (32–81 years old, mean: 52.9, STD: 13.6), and (iii) 15 healthy trained students forming the second reference set (23–25 years old, mean: 23.8, STD: 0.7). The MS Kinect used for data acquisition was installed about 60 cm above the floor. Each individual repeated a straight walk approximately 4 m long (5 steps) back and forth 5 times according to Fig. 4. The video record, acquired with a sampling

rate of 30 frames per second, contained useful information about the direct walk and undesirable frames recorded during the individuals' turns carrying no information about gait disorders.

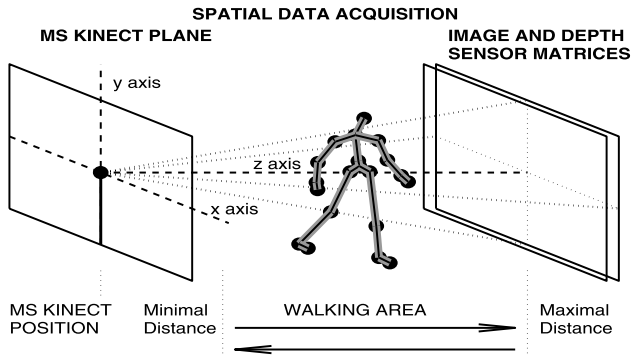

Fig. 4. Flowchart and the coordinate system for data acquisition using MS Kinect image and depth sensors.

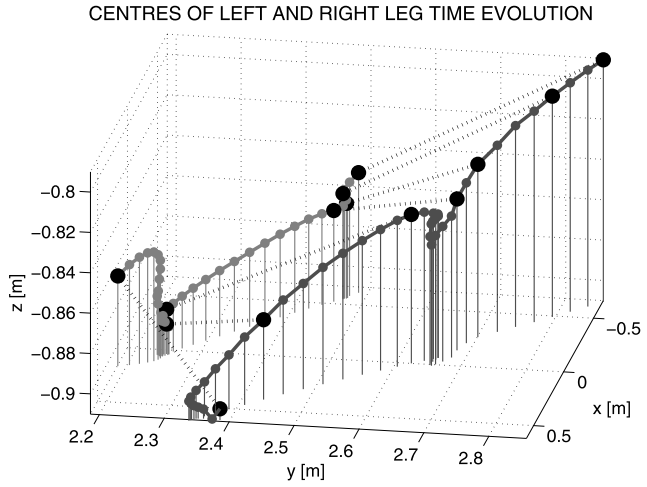

Fig. 5. The evolution of leg centers using data acquired by the MS Kinect and presentation of selected distances between leg centers used for estimation of stride lengths.

The range of the MS Kinect sensors did not allow continuous measurement of more steps in one direction and an algorithmic correction [25] after each walk segment was necessary. This limitation will occur in the new Kinect for Windows v2 as well even though its camera viewing angles are wider [46] and spatial resolution accuracy is higher.

2.2. Skeletal tracking

The skeletal tracking algorithm [24] processes the data acquired by the image and depth sensors to provide information about the location of the joints specified in Fig. 3(b) using the joint numbering and the connection map presented in Table 1.

The proposed algorithm for gait features detection using MS Kinect can be summarized into the following steps:

1. Preprocessing of skeleton data removing gross errors and filtering [47] of joint positions.
2. Rejection of frames with substantial errors using the time evolution of the centers of mass of joints 1–2–3.
3. Detection of segments of the gait in one direction.
4. Evaluation of the position of the centers of the legs (using joints 15–16 and 19–20) in each segment (Fig. 5) and estimation of the average step length using the Euclidean distances of the legs' centers, detecting their maxima.
5. Detection of the leg lengths of all individuals from skeleton data, evaluating the Euclidean distances between joints 13–14–15 and 17–18–19 of the left and right legs respectively (Fig. 6) and their averaging to normalize the stride length.
6. Estimation of the stride features, averaging the step length for each individual in each segment of the straight walk.

Further stride features, including the walk speed, can be detected in similar ways using the data of the MS Kinect image and depth sensors and three-dimensional coordinates of skeleton joints.

2.3. Bayesian classification

Suppose we have a matrix $\mathbf{X}_{N,R}$ of R features/attributes $\mathbf{x}_i$ (stride length, walking speed, age, ...) for each separate individual

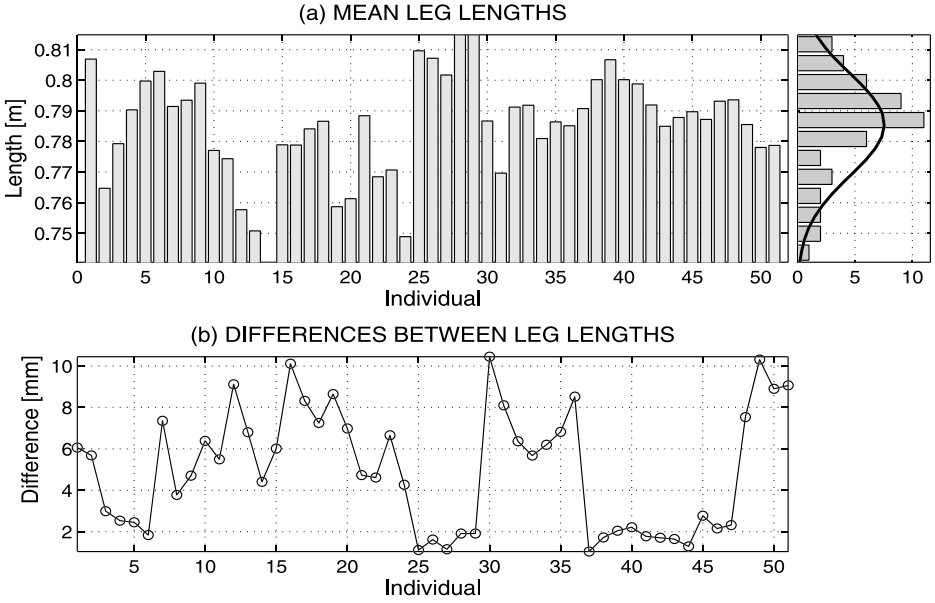

Fig. 6. Results of evaluation of leg lengths during the gait presenting (a) mean leg lengths for 51 individuals evaluated from data acquired by the MS Kinect sensors with histogram of their distribution and (b) differences between the length of the left and right legs of individuals evaluated from spatial positions of joints.

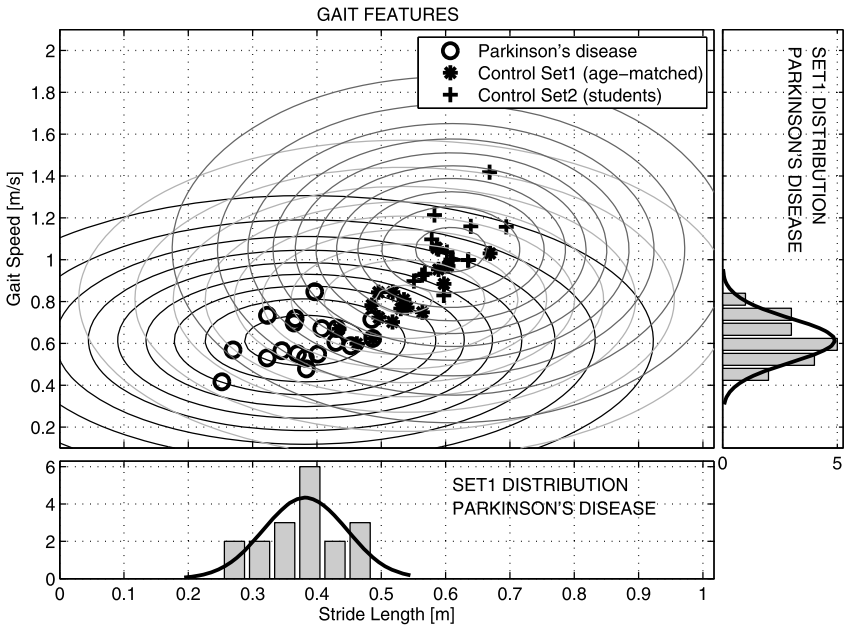

Fig. 7. Distribution of gait features (x_1 – stride length [m], x_2 – gait speed [m/s]) for three classes: 1) Parkinson's disease set, 2) the first control set (age-matched), 3) the second control set (students), and histograms of Parkinson's disease features.

$i = 1, 2, \cdots, N$. Let us define further the associated column vector $\mathbf{y}_{N,1}$ that specifies the class c_k, $k = 1, 2, \cdots, M$ of each individual selected from the given set of M classes. The set of these classes defines the gait quality evaluated by a neurologist, including, for instance: c_1 – individuals with Parkinson's disease, c_2 – normal age-matched controls, c_3 – normal trained persons. Fig. 7 presents the location of a selected pair of features. During the following learning process, a function that transforms the space of features $\mathbf{X}_{N,R}$ into the vector $\mathbf{y}_{N,1}$ specifying the classes is estimated.

The goal of the probabilistic classification is to find the estimate of class $\hat{c}_k$ of the unknown instance $\mathbf{x}$:

$$\hat{c}_k = max_{c_1,c_2,\cdots,c_M}(P(c_k\mathbf{x})) \tag{1}$$

The Bayesian probability [27,48] of an instance $\mathbf{x}$ being in class c_k, $k = 1, 2, \cdots, M$ is defined as

$$P(c_k\mathbf{x}) = \frac{P(\mathbf{x}c_k)\ P(c_k)}{P(\mathbf{x})} \tag{2}$$

where $P(\mathbf{x}c_k)$ stands for the probability of generating instance $\mathbf{x}$ given class c_k, $P(c_k)$ represents the probability of the occurrence of class c_k, and $P(\mathbf{x})$ stands for the probability of the occurrence of $\mathbf{x}$. This value can be normalized across all observations using the probabilities $P(c_k)$ of separate classes c_k:

$$P(\mathbf{x}) = \sum_{k=1}^{M} P(\mathbf{x}c_k)\ P(c_k) \tag{3}$$

where

$$P(c_k) = N_{c_k}/N \tag{4}$$

and N_{c_k} stands for the number of individuals belonging to class c_k.

Assuming the independence of continuous features and the Gaussian distribution of their values, it is possible to find for each class c_k the fundamental characteristics of each attribute x_j, including its mean μ_{c_k,x_j} and variance $\sigma^2_{c_k,x_j}$. The corresponding Gaussian distribution of each attribute x_j and each class c_k is then defined by

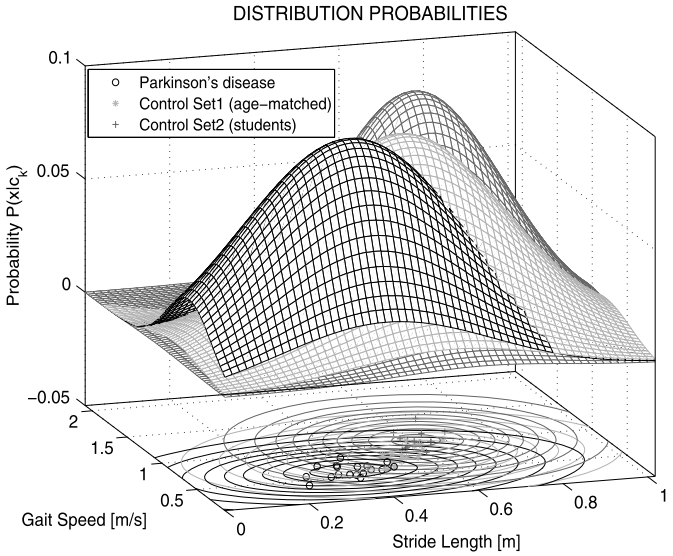

Fig. 8. Probabilities of individual classes related to gait features (x_1 – stride length [m], x_2 – gait speed [m/s]).

$$p(x_j c_k) = \frac{1}{\sqrt{2\,\pi\,\sigma^2_{c_k,x_j}}}\ \exp\left(-\frac{(x_j - \mu_{c_k,x_j})^2}{2\,\sigma^2_{c_k,x_j}}\right) \tag{5}$$

Fig. 7 presents this distribution for class c_1 of the individuals with Parkinson's disease.

For a class model it is possible to find how likely it is to see the observation $\mathbf{x}$ for class c_k by using the relation

$$P(\mathbf{x}c_k) = \prod_{j=1}^{R} p(x_j c_k). \tag{6}$$

The Bayesian probability of a class c_k is then defined by substituting Eq. (6) in Eq. (2). Fig. 8 presents three classes and individuals described by two features according to the observations specified above. The decision boundary separating the individual classes is formed by an ellipse, or in the general case by a parabolic or hyperbolic curve.

2.4. ROC analysis of gait features

The receiver operating characteristic (ROC) curves [49–51] can be used as an efficient tool for the evaluation of classification results [52]. The selected classifier finds in the negative set the number of true-negative individuals (TN) and the number of false-positive individuals (FP). In a similar way it finds in the positive set the number of true-positive individuals (TP) and the number of false-negative individuals (FN).

The associated performance metrics can then be used [52] to evaluate sensitivity ($SE = TP/(TP + FN)$, the true positive rate), specificity ($SP = TN/(TN + FP)$, the true negative rate) and accuracy as the probability of correct classification ($ACC = (TP + TN)/(TP + TN + FP + FN)$).

2.5. Methodology of Bayesian classification

The proposed algorithm for a Bayesian classifier consists of the following steps:

1. Determination of R features $[X(i,1), \cdots, X(i,R)]$ and associated classes $y(i,1)$ (selected from the set c_k, $k = 1, 2, \cdots, M$) for each individual $i = 1, 2, \cdots, N$;
2. Evaluation of the fundamental statistical measures (mean and standard deviation) associated with each class, specifying the (Gaussian) distribution of each attribute $X(i,j)$, $j = 1, 2, \cdots, R$ for rows i that belong to class c_k, $k = 1, 2, \cdots, M$ forming probability $p(x_j c_k)$ according to Eq. (5);
3. Evaluation of the probability $P(c_k)$ of the occurrence of class $c_k, k = 1, 2, \cdots, M$ using Eq. (4);
4. Estimation of the Bayesian probability of the unknown instance $\mathbf{x}$ (specified by features $[x_1, \cdots, x_R]$) being in class c_k, $k = 1, 2, \cdots, M$ according to Eq. (2) using Eqs. (6), (4) and (3), selection of the class with the highest probability and determination of the decision boundaries;
5. Evaluation of the numbers of estimated negative and positive individuals in the true negative and positive classes to find the selectivity, specificity and accuracy of the classification followed by cross-validation of the whole model.

Matrix $\mathbf{X}_{N,R}$ of R features can include the stride length, gait speed, and age in each its row. Corresponding column vector $\mathbf{y}_{N,1}$ contains classes specifying gait disorders resulting from medical examination of each individual by an expert (neurologist).

The simplicity of the Bayesian classification and the possibility of its graphical visualization contribute to its attractivity in many applications. It is one of the most efficient and effective learning algorithms for machine learning and selected empirical results summarized bellow show that naive Bayes predicts equally well as more sophisticated methods. Detail theoretical studies [53–55] explain reasons for optimality of the Bayes method under the Gaussian distribution and its use even in case that dependence between attributes do exist.

3. Results

Table 2 presents a summary of $R = 3$ features of $N = 51$ individual classified into the $M = 3$ classes: (i) c_1 – the Parkinson's disease set, (ii) c_2 – the first control set (age-matched), and (iii) c_3 – the second control set (students).

Results of estimating the leg lengths from the MS Kinect skeleton data for all individuals are presented in Fig. 6. The proposed algorithm is based upon the evaluation of the three-dimensional distances between the hip–knee and knee–ankle segments for the left and right legs in each frame of the direct walk, and their subsequent averaging. Fig. 6(a) presents the evaluated leg lengths of all $N = 51$ individuals and their distribution, with a mean value of 0.79 m. The mean difference between the lengths of the right and left legs found using the Kinect data is presented in Fig. 6(b). The range of these differences, 10 mm, with its mean value of 4 mm (and STD = 0.003) corresponds to common physiological norms. The values of the leg lengths were further used for normalization of the stride length and gait speed estimated from MS Kinect observations.

Table 2
Features (x_1 – stride length [m], x_2 – gait speed [m/s], x_3 – age [years]) and indices k of associated classes c_k: c_1 – Parkinson's disease, c_2 – control set (age-matched), c_3 – control set (students) of $N = 51$ individuals.

i	x_1	x_2	x_3	k	i	x_1	x_2	x_3	k
1	0.32	0.73	76	1	27	0.50	0.72	39	2
2	0.45	0.59	71	1	28	0.54	0.81	49	2
3	0.32	0.53	87	1	29	0.54	0.81	41	2
4	0.49	0.71	61	1	30	0.56	0.75	33	2
5	0.27	0.57	84	1	31	0.49	0.78	64	2
6	0.40	0.85	73	1	32	0.60	0.97	58	2
7	0.25	0.42	82	1	33	0.50	0.84	47	2
8	0.41	0.67	82	1	34	0.52	0.70	58	2
9	0.37	0.55	52	1	35	0.59	1.06	72	2
10	0.36	0.70	76	1	36	0.46	0.60	67	2
11	0.43	0.67	82	1	37	0.69	1.16	24	3
12	0.38	0.53	80	1	38	0.64	1.00	23	3
13	0.43	0.61	79	1	39	0.64	1.00	24	3
14	0.40	0.55	73	1	40	0.56	0.93	23	3
15	0.35	0.57	62	1	41	0.61	1.00	23	3
16	0.38	0.48	61	1	42	0.57	0.93	25	3
17	0.37	0.72	76	1	43	0.61	1.00	24	3
18	0.49	0.62	72	1	44	0.64	1.16	24	3
19	0.67	1.03	69	2	45	0.58	1.21	25	3
20	0.60	0.88	43	2	46	0.60	0.83	24	3
21	0.59	0.95	53	2	47	0.55	0.90	24	3
22	0.54	0.77	58	2	48	0.60	1.04	23	3
23	0.53	0.77	50	2	49	0.67	1.42	24	3
24	0.43	0.67	78	2	50	0.59	1.05	23	3
25	0.49	0.62	32	2	51	0.58	1.10	23	3
26	0.52	0.85	41	2					

Table 3
Characteristics of three classes c_k (c_1 – Parkinson's disease, c_2 – control set (age-matched), c_3 – control set (students)) and their features x_j (x_1 – stride length [m], x_2 – gait speed [m/s], x_3 – age [years]).

Class c_k			Feature					
			x_1 [m] Stride length		x_2 [m/s] Gait speed		x_3 [years] Age	
k	N_{c_k}	$P(c_k)$	μ_{c_k,x_1}	σ_{c_k,x_1}	μ_{c_k,x_2}	σ_{c_k,x_2}	μ_{c_k,x_3}	σ_{c_k,x_3}
1	18	0.35	0.38	0.07	0.61	0.12	73.8	9.4
2	18	0.35	0.54	0.06	0.81	0.15	52.9	13.6
3	15	0.30	0.61	0.04	1.05	0.15	23.8	0.7

The mean values and standard deviations of individual features x_i, $i = 1, 2, \cdots, R$ for separate classes c_k, $k = 1, 2, \cdots, M$ are summarized in Table 3. The resulting average stride lengths (feature x_1) resulting from MS Kinect data normalized to the average leg lengths formed one set of features for classifying individuals with Parkinson's disease (PD). The average stride length of the PD group $\mu_{c_1,x_1} = 0.38$ is shorter than that of the reference sets $\mu_{c_2,x_1} = 0.54$ and $\mu_{c_2,x_1} = 0.61$, as expected. The second feature (x_2) includes the estimated gait speed of the individuals summarized in Table 3 as well. The gait speed is the lowest for the PD group, as expected as well. The third feature (x_3) is the age of the individual.

Fig. 8 presents the probabilities of the separate classes related to 51 individuals classified into three sets according to features x_1 and x_2 by Eq. (6). Figs. 9(a, b) show how likely it is to see observation $\mathbf{x}$ in class c_1 – that of the Parkinson's disease individuals. The Bayesian probability of the instance $\mathbf{x}$ being in class c_1 is presented in Fig. 9(c) using Eq. (2) normalized by Eq. (3). In the given case,

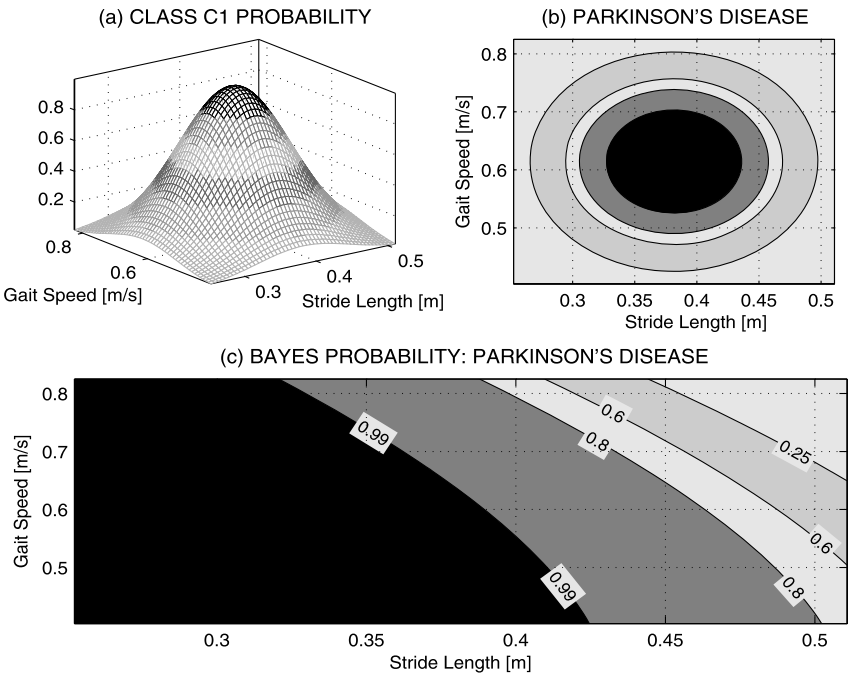

Fig. 9. Classification into class 1 (Parkinson's disease set) presenting (a) the 3D plot of Bayesian probabilities, (b) the contour plot related to the stride length [m] and gait speed [m/s] of the observed individuals, and (c) the detail part of this contour plot.

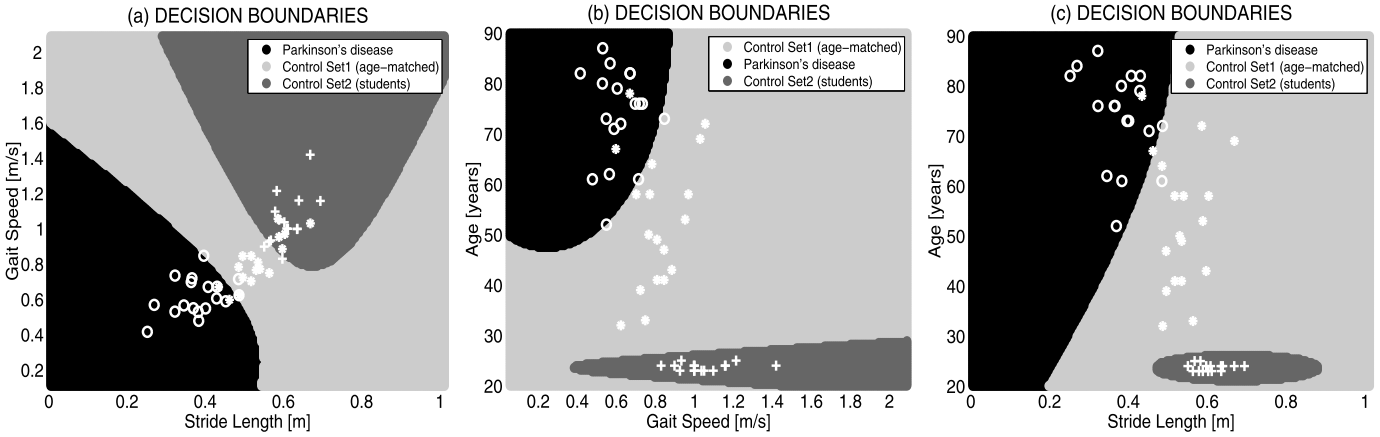

Fig. 10. Bayesian decision boundaries between individual classes: 1) Parkinson's disease set, 2) the first control set (age-matched), 3) the second control set (students), and the pair of attributes selected: (a) x_1 – stride length [m], x_2 – gait speed [m/s], (b) x_2 – gait speed [m/s], x_3 – age [years], and (c) x_1 – stride length [m], x_3 – age [years].

$P(c_1) = 18/51$. The complete set of characteristics of the separate classes is presented in Table 3.

The Bayesian decision boundaries between the individual classes are presented in Fig. 10, allowing the association of a pattern vector **x** with the most probable class for different couples of features: (a) x_1 – stride length [m], x_2 – gait speed [m/s], (b) x_2 – gait speed [m/s], x_3 – age [years], and (c) x_1 – stride length [m], x_3 – age [years]. These class boundaries can be used in clinical practice to suggest the classification of an individual into the most appropriate class.

The Bayesian probabilities evaluated from Eq. (2) for all individuals and selected feature couples were further used to find the optimal set of features and the classification accuracy. As clusters of features belonging to the trained young students (control set 2) are embedded into the areas of the features of control set 1 (healthy age-matched individuals) as presented in Fig. 10, both these sets form negative individuals.

Table 4
Results of classification into the positive class (c_1 – Parkinson's disease) and negative class (c_2 – control set (age-matched), c_3 – control set (students)) for selected couples of features (x_1 – stride length [m], x_2 – gait speed [m/s], x_3 – age [years]).

Features	Selectivity SE [%]	Specificity SP [%]	*Accuracy* ACC [%]
$x_1 - x_2$	94.4	92.2	92.2
$x_2 - x_3$	83.3	93.9	90.2
$x_1 - x_3$	94.4	93.9	94.1

The selectivity, specificity, and accuracy of the classification are summarized in Table 4 and show the highest accuracy of 94.1% for gait attributes including the stride length (x_1) and age (x_3) representing the best discrimination couple for the given set of individuals.

Present results [56] of age dependency of gait features prove that the linear regression has a decreasing trend in both features for the group of diseased subjects (gait speed: −0.01 m/s/year,

Table 5
Confusion matrices of classification into three classes c_k (c_1 – Parkinson's disease, c_2 – control set (age-matched), c_3 – control set (students)) using the leave-one-out scheme for features x_j (x_1 – stride length [m], x_2 – gait speed [m/s], x_3 – age [years]).

Target class	Output class								
	$x_1 - x_2$			$x_2 - x_3$			$x_1 - x_3$		
	c_1	c_2	c_3	c_1	c_2	c_3	c_1	c_2	c_3
c_1	15	3	0	15	3	0	16	2	0
c_2	3	10	5	2	16	0	2	16	0
c_3	0	4	11	0	0	15	0	0	15

stride length: −0.008 m/year) but there is no proved dependence on age for the healthy individuals.

The cross-validation [57,58] using the leave-one-out scheme resulted in the error rate values 0.118, 0.098, and 0.078 respectively, for features $x_1 - x_2$, $x_2 - x_3$ and $x_1 - x_3$ with the lowest value for features $x_1 - x_3$ (stride length-age) and the analysis of the positive set (PD subjects forming class c_1) versus negative set (individuals belonging to class c_2 and c_3). Numerical results presented in Table 5 are related to Figs. 10(a), (b), (c) and to analysis of separate feature couples.

4. Conclusion

The Microsoft Kinect is becoming increasingly used for human movement monitoring [9] and rehabilitation. Its reliability and accuracy are studied in many papers [18,25,60,40,61] now comparing its use and error bounds with more established techniques.

This paper presents a new approach to the analysis of gait disorders and Parkinson's disease recognition, using an inexpensive MS Kinect system. Its image and depth sensors with a spatial resolution of 4–40 mm are sufficient in the given case. The novelty of the paper is in (i) the processing of the data obtained through MS Kinect in the MATLAB computational environment using digital signal processing tools and (ii) a Bayesian evaluation of gait features to study the ability of MS Kinect sensors to follow movement disorders.

The results obtained prove that the proposed method is able to classify sets of individuals with an accuracy sufficient for distinguishing between the class of Parkinson's disease individuals and the control sets. The proposed algorithm includes a Bayesian classification of gait features into the selected class and the evaluation of the classification probability. This approach is valuable for clinical practice and the proposal of the most probable diagnosis. Bayesian methods provide a very useful mathematical tool in this way.

The comparison of the use of different features for gait disorder classification shows that all couples of features under study can be used for classification with an accuracy higher than 90%. The highest accuracy, 94.1%, was achieved for the stride length and age used as gait attributes for the given sets of individuals. Cross-validation for this pair of features resulted in the lowest error rate 0.078 as well.

More accurate results might be achieved using further features, including the level of movement coordination. The reliability of the results might be also increased for longer gait segments, as it was found in [59] that during about the first 30 steps, the gait quality increased for all sets of individuals.

Further classification algorithms [56,60] based upon artificial neural networks with sigmoidal and radial basis functions provided similar classification accuracy. The advantage of the Bayesian classification is in its simplicity and efficiency as it can also outperform more sophisticated classification methods [55] including the decision tree and k-nearest neighbor [62]. Selected results are presented in Table 6.

Table 6
Comparison of the Bayesian classification method with the decision tree and k-nearest neighbor (K-NN) classification using the leave-one-out scheme for cross-validation and features x_j (x_1 – stride length [m], x_2 – gait speed [m/s], x_3 – age [years]).

Classification method	Accuracy [%]			Cross-validation		
	$x_1 - x_2$	$x_2 - x_3$	$x_1 - x_3$	$x_1 - x_2$	$x_2 - x_3$	$x_1 - x_3$
Bayesian	92.2	92.2	94.1	0.08	0.12	0.08
Decision tree	94.1	92.2	94.1	0.06	0.08	0.08
3-NN	90.2	92.2	92.2	0.12	0.08	0.08
7-NN	90.2	86.3	86.3	0.12	0.16	0.15
10-NN	90.2	84.3	84.3	0.12	0.18	0.18

Future work will be devoted to the study of more extensive data sets, to the evaluation of further gait features, and to the study of their age dependency, in order to increase the accuracy of classification. It is assumed that further biosensors and appropriate data fusion methods will be used as well to contribute to the early diagnosis of gait disorders.

Acknowledgments

The authors would like to thank all the patients who signed the informed consent to participate in the project approved by the local ethics committee. All data were kindly acquired by the Movement Disorders Center of the Faculty Hospital in Hradec Králové, Czech Republic. The data processing and the use of Bayesian methods was strongly motivated by research work and personal contacts with Prof. Bill Fitzgerald at the University of Cambridge, the UK.

Appendix A. Supplementary material

Supplementary material related to this article can be found online at http://dx.doi.org/10.1016/j.dsp.2015.05.011.

References

[1] D. Barber, Bayesian Reasoning and Machine Learning, Cambridge University Press, 2012.
[2] F. Pernkopf, M. Wohlmayr, Stochastic margin-based structure learning of Bayesian network classifiers, Pattern Recognit. 46 (2013) 464–471.
[3] A. Kokaram, R.D. Morris, W. Fitzgerald, P.J.W. Rayner, Detection of missing data in image sequences, IEEE Trans. Image Process. 4 (1995) 1509–1519.
[4] M. Orton, W. Fitzgerald, A Bayesian approach to tracking multiple targets using sensor arrays and particle filters, IEEE Trans. Signal Process. 59 (2) (2002) 216–223.
[5] J.W. Yoon, A. Bruckbauer, W. Fitzgerald, D. Klenerman, Bayesian inference for improved single molecule fluorescence tracking, Biophys. J. 94 (12) (2008) 4932–4947.
[6] K. Kayabol, E.E. Kuruoglu, B. Sankur, Bayesian separation of images modeled with MRFs using MCMC, IEEE Trans. Image Process. 18 (5) (2009) 982–994.
[7] J.J.K. Ruanaidh, W.J. Fitzgerald, Numerical Bayesian Methods Applied to Signal Processing, Springer-Verlag, New York, 1996.
[8] M. Gabel, E. Renshaw, A. Schuster, R. Gilad-Bachrach, Full body gait analysis with Kinect, in: Int. Conference of the IEEE Engineering in Medicine and Biology, 2012, pp. P1–P4.
[9] J. Preis, M. Kessel, M. Werner, C. Linnhoff-Popien, Gait recognition with Kinect, in: 1st International Workshop on Kinect in Pervasive Computing, Newcastle, 2012, pp. P1–P4.
[10] D. Gelb, E. Oliver, S. Gilman, Diagnostic criteria for Parkinson disease, JAMA Neurol. 56 (1) (1999) 33–39.
[11] G. Yogev, N. Giladi, C. Peretz, S. Springer, E.S. Simon, J.M. Hausdorff, Dual tasking, gait rhythmicity, and Parkinson's disease: which aspects of gait are attention demanding?, Eur. J. Neurosci. 22 (5) (2005) 1248–1256.
[12] U. Dillmann, C. Holzhoffer, Y. Johann, S. Bechtel, S. Graber, C. Massing, J. Spiegel, S. Behnke, J. Burmann, A.K. Louis, Principal component analysis of gait in Parkinson's disease: relevance of gait velocity, Gait Posture 39 (2014) 882–887.
[13] R.R. Bouckaert, Naive Bayes classifiers that perform well with continuous variables, in: AI 2004, in: Lecture Notes in Computer Science, vol. 3339, 2004, pp. 1089–1094.
[14] F. Stella, Y. Amer, Continuous time Bayesian network classifiers, J. Biomed. Inform. 45 (6) (2012) 1108–1119.

[15] J. Lasenby, A. Stevenson, Using geometric algebra for optical motion capture, in: E. Bayro-Corrochano, G. Sobcyzk (Eds.), Applied Clifford Algebras in Computer Science and Engineering, Birkhäuser, Boston, USA, 2000.
[16] M. Ringer, J. Lasenby, Multiple hypothesis tracking for automatic optical motion capture, in: ECCV 2002, in: Lecture Notes in Computer Science, vol. 2350, 2002, pp. 524–536.
[17] A. Procházka, M. Kubíček, A. Pavelka, Multicamera systems in the moving body recognition, in: International Symposium ELMAR-2006, 2006, pp. 280–282.
[18] R.A. Clark, Y.H. Pua, K. Fortin, C. Ritchie, K.E. Webster, L. Denehy, A.L. Bryant, Validity of the Microsoft Kinect for assessment of postural control, Gait Posture 36 (2012) 372–377.
[19] M. Milovanovic, M. Minovic, D. Starcevic, New gait recognition method using Kinect stick figure and CBIR, in: Telecommunications Forum 2012, pp. 1323–1326.
[20] I. Weber, J. Koch, J. Meskemper, K. Friedl, K. Heinrich, U. Hartmann, Is the MS Kinect suitable for motion analysis?, Biomed. Eng. 57 (2012) 664.
[21] M. Strbac, M. Markovic, D.B. Popovic, Kinect in neurorehabilitation: computer vision system for real time hand and object detection and distance estimation, in: The 11th Symposium on Neural Network Application in Electrical Engineering 2012, IEEE, USA, 2012, pp. 127–132.
[22] C. Zhang, J. Xu, N. Xi, Y. Jia, W. Li, Development of an omni-directional 3D camera for robot navigation, in: The 2012 IEEE/ASME International Conference on Advanced Intelligent Mechatronics, USA, 2012, pp. 262–267.
[23] E. Machida, M. Cao, T. Murao, H. Hashimoto, Human motion tracking of mobile robot with Kinect 3D sensor, in: SICE Annual Conference, Akita Univ., Japan, 2012, pp. 2207–2211.
[24] J. Shotton, A. Fitzgibbon, M. Cook, T. Sharp, M. Finocchio, R. Moore, A. Kipman, A. Blake, Real-time human pose recognition in parts from single depth images, in: Machine Learning for Computer Vision, Springer-Verlag, Berlin, 2013, pp. 119–135.
[25] B. Galna, G. Barry, D. Jackson, D. Mhiripiri, P. Olivier, L. Rochester, Accuracy of the Microsoft Kinect sensor for measuring movement in people with Parkinson's disease, Gait Posture 39 (2014) 1062–1068.
[26] J.L. Raheja, A. Chaudhary, K. Nandhini, S. Maiti, Pre-consultation help necessity detection based on gait recognition, Signal Image Video Process. 8 (2014) P1–P7.
[27] C.M. Bishop, Pattern Recognition and Machine Learning, Springer-Verlag, Berlin, 2006.
[28] W.J. Fitzgerald, J.J.K.O. Ruanaidh, Generalized change point detection, Tech. rep. CUED/F-INFENG/TR 187, University of Cambridge, Department of Engineering, 1994.
[29] P.J.W. Rayner, W.J. Fitzgerald, The Bayesian approach to signal modeling and classification, in: A. Procházka, J. Uhlíř, P.J.W. Rayner, N.G. Kingsbury (Eds.), Signal Analysis and Prediction, Birkhäuser, 1998, Ch. 9.
[30] A.H. Ham, W.J. Fitzgerald, Unsupervised multiscale image segmentation, in: The 10th International Conference on Image Analysis and Processing, ICIAP'99, IEEE Computer Society, 1998, pp. 316–321.
[31] W.J. Fitzgerald, S.J. Godsill, A.C. Kokaram, A. Stark, Bayesian methods in signal and image processing, in: Bayesian Statistics 6: Proc. of the 11th Conf. on Uncertainty in Artificial Intelligence, Oxford University Press, 1998, pp. 239–254.
[32] M. Costagli, E.E. Kuruoglu, Image separation using particle filters, Digit. Signal Process. 17 (5) (2007) 935–946.
[33] A.T. Cemgil, C. Févotte, S.J. Godsill, Variational and stochastic inference for Bayesian source separation, Digit. Signal Process. 17 (5) (2007) 891–913.
[34] L.S. de Oliveira, R.V. Andreao, M. Sarcinelli-Filho, The use of Bayesian networks for heart beat classification, Adv. Exp. Med. Biol. 657 (2010) 217–231.
[35] D.S. Medhekar, M.P. Bote, S.D. Deshmukh, Heart disease prediction system using naive Bayes, Int. J. Enhanc. Res. Sci. Technol. Eng. 2 (3) (2013) 1–5.
[36] H. Hiary, R.S. Alomari, M. Saadah, V. Chaudhary, Automated segmentation of stromal tissue in histology images using a voting Bayesian model, Signal Image Video Process. 7 (6) (2013) 1229–1237.
[37] M. Yu, Y. Yu, A. Rhuma, S.M.R. Naqvi, L. Wang, J.A. Chambers, An online one class support vector machine-based person-specific fall detection system for monitoring an elderly individual in a room environment, IEEE J. Biomed. Health Inform. 17 (6) (2013) 1002–1014.
[38] Y. Wang, C. Yang, X. Wu, S. Xu, H. Li, Kinect based dynamic hand gesture recognition algorithm research, in: The 4th International Conference on Intelligent Human–Machine Systems and Cybernetics, 2012, pp. 274–279.
[39] K. Essmaeel, L. Gallo, E. Damiani, G. De Pietro, A. Dipanda, Temporal denoising of Kinect depth data, in: The Eighth International Conference on Signal Image Technology and Internet Based Systems, IEEE Computer Society, 2012, pp. 47–52.
[40] S. Obdrzalek, G. Kurillo, F. Ofli, R. Bajcsy, E. Seto, H. Jimison, M. Pavel, Accuracy and robustness of Kinect pose estimation in the context of coaching of elderly population, in: The 34th Annual International Conference of the IEEE EMBS, USA, 2012, pp. 1188–1193.
[41] Y. Li, Multi-scenario gesture recognition using Kinect, in: The 17th Int. Conference on Computer Games, 2012, pp. 126–130.
[42] J. Smisek, M. Jancosek, T. Pajdla, 3D with Kinect, in: IEEE Int. Conference on Computer Vision, USA, 2012, pp. 1154–1160.
[43] A. Staranowicz, G. Brown, G.L. Mariottini, Evaluating the accuracy of a mobile Kinect-based gait-monitoring system for fall prediction, in: Proceedings of the 6th International Conference on Pervasive Technologies Related to Assistive Environments, PETRA '13, ACM, 2013, pp. P1–P4.
[44] Z. Zhang, Accuracy and resolution of Kinect depth data for indoor mapping applications, IEEE Multimed. 19 (2) (2012) 4–10.
[45] S. Qin, X. Zhu, Y. Yang, Real-time hand gesture recognition from depth images using convex shape decomposition method, J. Signal Process. Syst. 74 (2014) 47–58.
[46] C. Amon, F. Fuhrmann, Evaluation of the spatial resolution accuracy of the face tracking system for Kinect for Windows v1 and v2, in: The 6th Congress of Alps–Adria Acoustics Association, Graz, Austria, 2014, pp. P1–P4.
[47] N. Kingsbury, J. Mugarey, Wavelet transforms in image processing, in: A. Prochazka, J. Uhlir, P.J.W. Rayner, N. Kingsbury (Eds.), Signal Analysis and Prediction, Birkhäuser, 1998.
[48] O.D. Duda, P.E. Hart, D.G. Stork, Pattern Classification, John Wiley & Sons, New York, USA, 2001.
[49] J.A. Hanley, B.J. McNeil, The meaning and use of the area under a receiver operating characteristic (ROC) curve, Radiology 143 (1982) 29–36.
[50] M.H. Zweig, G. Campbell, Receiver-operating characteristic (ROC) plots: a fundamental evaluation tool in clinical medicine, Clin. Chem. 39 (1993) 561–577.
[51] T. Fawcett, An introduction to ROC analysis, Pattern Recognit. Lett. 27 (2006) 861–874.
[52] A. Procházka, O. Vyšata, O. Ťupa, M. Yadollahi, M. Vališ, Discrimination of axonal neuropathy using sensitivity and specificity statistical measures, Neural Comput. Appl. 25 (6) (2014) 1349–1358, http://dx.doi.org/10.1007/s00521-014-1622-0.
[53] H. Zhang, Exploring conditions for the optimality of naive Bayes, Int. J. Pattern Recognit. Artif. Intell. 19 (2) (2005) 183–192.
[54] N.A. Zaidi, J. Cerquides, M.J. Carman, G.I. Webb, Alleviating naive Bayes attribute independence assumption by attribute weighting, J. Mach. Learn. Res. 14 (2013) 1947–1988.
[55] A. Ashari, I. Paryudi, A.M. Tjoa, Performance comparison between naive Bayes, decision tree and k-nearest neighbor in searching alternative design in an energy simulation tool, Int. J. Adv. Comput. Sci. Appl. 4 (11) (2013) 33–39.
[56] O. Tupa, Multi-dimensional data modelling and analysis using MS KINECT, Master thesis, ICT Prague, 2014.
[57] S. Haykin, Neural Networks and Learning Machines, Pearson International, 2009.
[58] S. Ounpraseuth, S.Y. Lensing, J.H. Spencer, R.L. Kodell, Estimating misclassification error: a closer look at cross-validation based methods, BMC Res. Notes 5 (2012) 656.
[59] B. Galna, S. Lord, L. Rochester, Is gait variability reliable in older adults and Parkinson's disease? Towards an optimal testing protocol, Gait Posture 37 (2013) 580–585.
[60] A. Procházka, O. Vyšata, M. Schätz, O. Ťupa, M. Yadollahi, M. Vališ, The MS Kinect image and depth sensors use for gait features detection, in: The IEEE Int. Conf. on Image Processing, ICIP, 2014, pp. 2271–2274.
[61] H.M. Hondori, M. Khademi, A review on technical and clinical impact of Microsoft Kinect on physical therapy and rehabilitation, J. Biomed. Eng. (2014) P1–P16, http://dx.doi.org/10.1155/2014/846514, Article ID 846514.
[62] M.J. Islam, Q.M.J. Wu, M. Ahmadi, M.A. Sid-Ahmed, Investigating the performance of naive Bayes classifiers and k-nearest neighbor classifiers, J. Converg. Inf. Technol. 5 (2) (2010) 133–137.

Aleš Procházka received the Ph.D. in 1983 and has been appointed as a professor in Technical Cybernetics by the Czech Technical University in 2000. Since 1980 he has been the Head of the Digital Signal and Image Processing Research Group with interests in computational intelligence, mathematical methods of multidimensional data analysis, and image processing. His further research interests include segmentation, feature extraction and classification in biomedical and engineering applications.

Oldřich Vyšata received the M.D. in 1985 from the Medical Faculty of the University of J.E. Purkyně and the Ph.D. in Technical Cybernetics in 2011. He is a member of the European Neurological Society, the Czech Society of Clinical Neurophysiology, the Czech League Against Epilepsy, the Czech Medical Association of J.E. Purkyně, and the Gait and Clinical Movement Analysis Society (GCMAS). He is oriented towards computational medicine, digital signal processing, and artificial intelligence.

Martin Vališ completed his doctoral studies in neurology at the Medical faculty of Masaryk University in 2009. In 2012 he obtained the position of Associate Professor in neurology at the Charles University. Currently he is the Head of the Department of Neurology at the Medical Faculty of Charles University in Hradec Králové and his research and educational interests include the study of Parkinson's disease, diabetic polyneuropathy, and dementia problems related to age.

Ondřej Ťupa received his M.Sc. degree in Process Engineering and Informatics from the Institute of Chemical Technology in Prague in 2014. After his stay at Brunel University in London he is currently a research students and a member of the Digital Signal and Image Processing Research Group at the Department of Computing and Control Engineering in Prague. His research focuses on biomedical signal analysis, segmentation, feature extraction and classification.

Martin Schätz received his B.Sc. degree in Process Engineering and Informatics in 2013. At present he is a member of the Digital Signal and Image Processing Research Group at the Department of Computing and Control Engineering and a student at the Institute of Chemical Technology in Prague. His research interests include analysis of video sequences for movement recognition, data acquisition, fusion of signals from different sensors and their processing for image components detection.

Vladimír Mařík received his M.Sc. and Ph.D. degrees in artificial intelligence at the Czech Technical University, Prague. He is a director of the Czech Institute of Informatics, Robotics and Cybernetics of the Czech Technical University. His research interests are in artificial intelligence, multiagent systems, soft-computing, computational intelligence, production planning, and computer-integrated manufacturing applications.